CONEM 2016
CONGRESSO NACIONAL DE ENGENHARIA MECÂNICA
ABCM 40 anos
Associação Brasileira de Engenharia e Ciências Mecânicas
21 - 25 AGOSTO DE 2016
FORTALEZA - CEARÁ

MODEL PREDICTIVE CONTROLLER USED IN GUIDANCE WITH OBSTACLE AVOIDANCE OF MULTIROTOR AERIAL VEHICLES

José Agnelo Bezerra Guilherme Silva, agnelo@ita.br[1]
Davi Antônio dos Santos, davists@ita.br[1]
[1]Instituto Tecnológico de Aeronáutica (ITA), Praça Mal. Eduardo Gomes, 50, Vila das Acácias, São José dos Campos-SP

Abstract: *This article deals with the problem of waypoint-based guidance of multirotor aerial vehicles with avoidance of multiple polytopic obstacles. In order to solve the problem, a formulation of a model predictive controller (MPC) is proposed. The command inputs to the controller consist of a sequence of tridimensional waypoints as well as a reference speed. In the case with no obstacles close to the multirotor, the future reference trajectory embedded in the MPC is chosen as a straight line, traveled with the reference speed, towards the next waypoint of the sequence. A waypoint is detected as soon as the vehicle enters inside a specified Euclidean ball centered at it. At the same moment, the next waypoint of the sequence is switched on. This rule is repeated until reaching the final waypoint, at which the vehicle is commanded to hover. When a polytopic obstacle is close to the vehicle, the avoidance method is activated with two independent actions: a constant deceleration is introduced in the reference trajectory and the convex optimization space to MPC is reduced based on a simple method that considers both the previous and next waypoints. The proposed method is evaluated using a Monte Carlo scheme, showing that its effectiveness in guiding a multirotor vehicle in the presence of multiple obstacles, even subjected to parametric uncertainties and under aleatory disturbance forces.*
Keywords: *Model Predictive Control, Multirotor Aerial Vehicles, Waypoint Navigation, Obstacle Avoidance*

1. Introduction

Waypoint-based guidance for multirotor aerial vehicles is already a popular technology, being available even in open-source/open-hardware autopilots systems, such as the Mission Planner/Ardupilot Mega. Basically, it consists in controlling the position of a vehicle so as to make it approximately pass through desired positions, which we call waypoints.

The model predictive control (MPC) strategy has proven quite suitable for both trajectory planning and guidance of aerial vehicles [Richards and How (2002)], since it can carry out those tasks in an optimal sense, while considering the existence of constraints on position, velocity, and acceleration. The paper Almeida (2008) investigates the constrained infinite horizon model predictive control approach in a tridimensional waypoint navigation problem, considering flight and engine limitations. Raffo *et al.* (2010) uses a hierarchical control setting consisting of a predictive controller for the trajectory tracking in the outer loop and a nonlinear $\mathcal{H}_\infty$ controller for the attitude control in the inner loop. The paper tests this arrangement with numerical simulations, which assures robustness against external disturbances, parametric and structural uncertainties of the model. In Alexis *et al.* (2014), the authors employ a Robust MPC formulation with the metric of Minimum Peak Performance Measure. Bounded unknown disturbances are considered in the control modeling and the robustness of this strategy is noticed by means of a batch of experiments.

The reference Viana *et al.* (2015) dealt with the position control of a multirotor helicopter with deviation from a static obstacle. The referred paper used a MPC strategy set as a mixed-integer quadratic programming (MIQP) problem. The obstacle avoidance was carried out by the authors with a group of linear inequalities containing some boolean design variables, which responds about the mixed character of the optimization problem. The present work faces the obstacle avoidance problem with linear inequalities in terms of the quadrotor's position. Therewith, the resulting optimization problem is a simpler quadratic programming (QP) formulation of MPC. Moreover this approach allows the deviation from multiple polytopic obstacles that lies in the flight environment without any major increase of final problem's complexity.

The remaining text is organized in the following manner. Section 2 enunciates the waypoint-based multirotor guidance problem. Section 3 presents an MPC for solving the guidance problem defined in Section 2. Section 4 shows the simulation results. Finally, Section 5 presents the concluding remarks.

2. Problem Definition

Consider a multirotor aerial vehicle and two Cartesian Coordinate Systems (CCS), which are illustrated in Fig. 1. The body CCS $S_{\mathrm{B}} = \{X_{\mathrm{B}}, Y_{\mathrm{B}}, Z_{\mathrm{B}}\}$ is fixed on the vehicle's frame at its center of mass (CM). The ground CCS $S_{\mathrm{G}} = \{X_{\mathrm{G}}, Y_{\mathrm{G}}, Z_{\mathrm{G}}\}$ is fixed on a known point on Earth. For simplicity, the time dependence of all vectors that will appear from now on in the text will not be denoted explicitly.

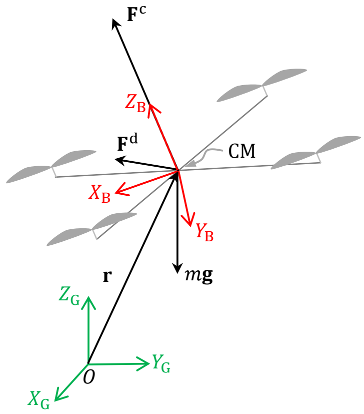

Figura 1: **Cartesian Coordinate Systems and forces in a multirotor aerial vehicle.**

Assume that S_{G} is an inertial frame. In this case, an immediate application of the second Newton's law gives the following dynamics model for the translational motion of the vehicle represented in S_{G}:

$$\ddot{\mathbf{r}}_{\mathrm{G}} = \frac{1}{m}\left(\mathbf{F}^{\mathrm{c}}_{\mathrm{G}} + \mathbf{F}^{\mathrm{d}}_{\mathrm{G}}\right) + \mathbf{g}_{\mathrm{G}}, \tag{1}$$

$$\mathbf{F}^{\mathrm{c}}_{\mathrm{G}} = \mathbf{D}^{\mathrm{T}}\mathbf{F}^{\mathrm{c}}_{\mathrm{B}}, \tag{2}$$

where $\mathbf{r}_{\mathrm{G}} \in \mathbb{R}^3$ denotes the position $\mathbf{r}$ of CM represented in S_{G}; $\mathbf{F}^{\mathrm{c}}_{\mathrm{G}}, \mathbf{F}^{\mathrm{c}}_{\mathrm{B}} \in \mathbb{R}^3$ are the total thrust force vector $\mathbf{F}^{\mathrm{c}}$ represented in S_{G} and S_{B}, respectively; $\mathbf{F}^{\mathrm{d}}_{\mathrm{G}} \in \mathbb{R}^3$ is the disturbance force vector $\mathbf{F}^{\mathrm{d}}$ represented in S_{G}; $\mathbf{g}_{\mathrm{G}} \triangleq \begin{bmatrix} 0 & 0 & -g \end{bmatrix}^{\mathrm{T}}$ is the gravitational acceleration vector represented in S_{G}, with g denoting its magnitude; m is the mass of the vehicle; and $\mathbf{D} \in SO(3)$ is the attitude matrix representing the attitude of S_{B} w.r.t. S_{G}.

Define the jth waypoint $\mathbf{w}_{\mathrm{j}} \in \mathbb{R}^3$ as a position vector represented in S_{G}. Assume that a sequence $\{\mathbf{w}_1, \mathbf{w}_2, ..., \mathbf{w}_{\mathrm{q}}\}$ of q waypoints is known beforehand. Consider the specification of a reference speed $\bar{v} \in \mathbb{R}_+$ for the vehicle's trajectory. Therefore, define the reference trajectory $\bar{\mathbf{r}}$ of the vehicle's flight as the sequence of line segments linking the waypoints, traveled with initial speed $\bar{v}$ (see Fig. 2).

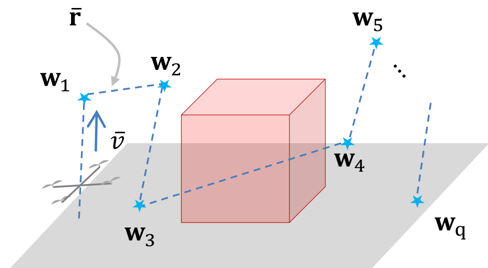

Figura 2: **A waypoint-based reference trajectory in an environment containing a polytopic obstacle.**

Assume that the vehicle is restricted to fly inside a bounded environment described by

$$\mathbf{r}_{\min} \leq \mathbf{r}_{\mathrm{G}} \leq \mathbf{r}_{\max}, \tag{3}$$

where $\mathbf{r}_{\min}, \mathbf{r}_{\max} \in \mathbb{R}^3$ are given limiting positions.

Furthermore, consider that this environment contains multiple polytopic obstacles, which can be described in the form of linear inequalities, as follows:

$$\boldsymbol{\Theta}^{\mathrm{i}}\check{\mathbf{r}} \leq \boldsymbol{\theta}^{\mathrm{i}}, \tag{4}$$

with $\mathbf{\Theta}^{\mathrm{i}} \in \mathbb{R}^{n_s \times 3}$, $\boldsymbol{\theta}^{\mathrm{i}} \in \mathbb{R}^{n_s}$, where n_s is the number of sides of the obstacle and $\check{\mathbf{r}}$ is a generic position vector satisfying the environment described by 3.

In order to respect the maximal thrust limit of the rotors, avoid inadvertent flips, and maintain all the rotors rotating without stopping, consider the following thrust force constraints:

$$\mathbf{F}_{\mathrm{min}} \leq \mathbf{F}_{\mathrm{G}}^{\mathrm{c}} \leq \mathbf{F}_{\mathrm{max}}, \tag{5}$$

where $\mathbf{F}_{\mathrm{min}}, \mathbf{F}_{\mathrm{max}} \in \mathbb{R}^3$ are given limiting thrust forces. For more details about position control under thrust constraints, see the reference Santos *et al.* (2013).

Problem 1. The waypoint-based guidance problem for multirotor aerial vehicles is to find a feedback control law for $\mathbf{F}_{\mathrm{G}}^{\mathrm{c}}$ that makes the vehicle's position $\mathbf{r}_{\mathrm{G}}$ follow the reference trajectory $\bar{\mathbf{r}}$ in the presence of a constant wind ($\mathbf{F}_{\mathrm{G}}^{\mathrm{d}}$), while respecting the environment constraint in (3), the thrust constraint in (5) and avoiding the obstacles described by (4).

3. Problem Solution

This section presents a solution to Problem 1 based on a traditional state-space formulation of MPC (which can be found on Maciejowski (2002)).

3.1 Preliminary Considerations

The method presented in this section considers the following two assumptions.

Assumption 1. The vehicle is not subject to force disturbances.

Assumption 2. Let $\bar{\mathbf{F}} \in \mathbb{R}^3$ denote the thrust command computed by the guidance law defined in Problem 1. Assume that $\mathbf{F}_{\mathrm{G}}^{\mathrm{c}} \equiv \bar{\mathbf{F}}$.

Considering Assumptions 1-2, a design model can be immediately obtained from equation (1) as:

$$\ddot{\mathbf{r}}_{\mathrm{G}} = \frac{1}{m}\bar{\mathbf{F}} + \mathbf{g}_{\mathrm{G}}. \tag{6}$$

3.2 State-Space Model and Constraints

Define the state vector $\mathbf{x} \triangleq \left[\mathbf{r}_{\mathrm{G}}^{\mathrm{T}}\ \dot{\mathbf{r}}_{\mathrm{G}}^{\mathrm{T}}\right]^{\mathrm{T}}$, the controlled output vector $\mathbf{y} \triangleq \mathbf{r}_{\mathrm{G}}$, and the control input vector

$$\mathbf{u} \triangleq \frac{1}{m}\bar{\mathbf{F}} + \mathbf{g}_{\mathrm{G}}. \tag{7}$$

From equations (6)-(7), one can describe the translational dynamics of the vehicle by the following discrete-time linear time-invariant state-space model:

$$\mathbf{x}_{\mathrm{k}+1} = \mathbf{A}\mathbf{x}_{\mathrm{k}} + \mathbf{B}\mathbf{u}_{\mathrm{k}}, \tag{8}$$

$$\mathbf{y}_{\mathrm{k}} = \mathbf{C}\mathbf{x}_{\mathrm{k}}, \tag{9}$$

with

$$\mathbf{A} = \begin{bmatrix} \mathbf{I}_3 & T\mathbf{I}_3 \\ \mathbf{0}_{3\times 3} & \mathbf{I}_3 \end{bmatrix} \in \mathbb{R}^{6\times 6},\ \mathbf{B} = \begin{bmatrix} \frac{T^2}{2}\mathbf{I}_3 \\ T\mathbf{I}_3 \end{bmatrix} \in \mathbb{R}^{6\times 3},\ \mathbf{C} = \begin{bmatrix} \mathbf{I}_3 & \mathbf{0}_{3\times 3} \end{bmatrix} \in \mathbb{R}^{3\times 6},$$

where T is the sample time.

Consider the augmented state vector as $\mathbf{z}_{\mathrm{k}} \triangleq \left[\Delta\mathbf{x}_{\mathrm{k}}^{\mathrm{T}}\ \mathbf{y}_{\mathrm{k}}^{\mathrm{T}}\right]^{\mathrm{T}} \in \mathbb{R}^9$, where $\Delta\mathbf{x}_{\mathrm{k}} \triangleq \mathbf{x}_{\mathrm{k}} - \mathbf{x}_{k-1}$. Using this definition, the model in (8)-(9) can be manipulated to a incremental formulation:

$$\mathbf{z}_{\mathrm{k}+1} = \tilde{\mathbf{A}}\mathbf{z}_{\mathrm{k}} + \tilde{\mathbf{B}}\Delta\mathbf{u}_{\mathrm{k}}, \tag{10}$$

$$\mathbf{y}_{\mathrm{k}+1} = \tilde{\mathbf{C}}\mathbf{z}_{\mathrm{k}+1}, \tag{11}$$

where $\Delta\mathbf{u}_{\mathrm{k}} \triangleq \mathbf{u}_{\mathrm{k}} - \mathbf{u}_{\mathrm{k}-1}$ and

$$\tilde{\mathbf{A}} \triangleq \begin{bmatrix} \mathbf{A} & \mathbf{0}_{6\times 3} \\ \mathbf{CA} & \mathbf{I}_3 \end{bmatrix} \in \mathbb{R}^{9\times 9},\ \tilde{\mathbf{B}} \triangleq \begin{bmatrix} \mathbf{B} \\ \mathbf{CB} \end{bmatrix} \in \mathbb{R}^{9\times 3},\ \tilde{\mathbf{C}} \triangleq \begin{bmatrix} \mathbf{0}_{3\times 6} & \mathbf{I}_3 \end{bmatrix} \in \mathbb{R}^{3\times 9}.$$

From the definition of $\mathbf{y}$, the constraint given in 3 can be rewritten as

$$\mathbf{r}_{\mathrm{min}} \leq \mathbf{y}_{\mathrm{k}} \leq \mathbf{r}_{\mathrm{max}}. \tag{12}$$

Finally, using Assumption 2 and equation (7), the constraint given in 5 can be written in terms of $\mathbf{u}_{\mathrm{k}}$, resulting:

$$\mathbf{u}_{\mathrm{min}} \leq \mathbf{u}_{\mathrm{k}} \leq \mathbf{u}_{\mathrm{max}}, \tag{13}$$

where $\mathbf{u}_{\mathrm{min}}$ and $\mathbf{u}_{\mathrm{max}}$ are computed using equation 7, but replacing $\bar{\mathbf{F}}$ by $\mathbf{F}_{\mathrm{min}}$ and $\mathbf{F}_{\mathrm{max}}$, respectively.

3.3 Obastacle Avoidance

In order to avoid the obstacles described by (4), we propose the following strategy, which is implemented for each polytope:

1. Define the obstacle perception radius $\beta \in \mathbb{R}_+$ as a design parameter. To account for the ith obstacle, we establish the condition

$$d_{\mathrm{k}}^{\mathrm{i}} \leq \beta, \tag{14}$$

where

$$d_{\mathrm{k}}^{\mathrm{i}} = \min_{\mathbf{\Theta}^{\mathrm{i}}\check{\mathbf{r}} \leq \boldsymbol{\theta}^{\mathrm{i}}} \|\check{\mathbf{r}} - \mathbf{r}_{\mathrm{k}}\|. \tag{15}$$

If the condition of (14) is not verified, the obstacle is simply ignored by the position controller.

2. Consider that the next waypoint of the sequence is $\mathbf{w}_{\mathrm{j}}$ and the current time instant is k. Define the sth external side of the obstacle as follows:

$$\mathcal{I}_{\mathrm{s}}^{\mathrm{i}} \triangleq \left\{\check{\mathbf{r}} : -\mathbf{\Theta}_{\mathrm{s}}^{\mathrm{i}}\check{\mathbf{r}} \leq -\theta_{\mathrm{s}}^{\mathrm{i}}\right\}, \tag{16}$$

where $\mathbf{\Theta}_{\mathrm{s}}^{\mathrm{i}}$ is the sth line of $\mathbf{\Theta}^{\mathrm{i}}$ and $\theta_{\mathrm{s}}^{\mathrm{i}}$ is the sth component of $\boldsymbol{\theta}^{\mathrm{i}}$.

With this, in the case of $d_{\mathrm{k}}^{\mathrm{i}} \leq \beta$, the vehicle's position is limited to the external spaces that contain both the previous ($\mathbf{w}_{\mathrm{j}-1}$) and the next waypoint $\mathbf{w}_{\mathrm{j}}$. So, the obstacle constraint is given as follows:

$$-\mathbf{\Theta}_{s}^{\mathrm{i}}\mathbf{y}_{\mathrm{k}} \leq -\theta_{s}^{\mathrm{i}}. \tag{17}$$

The strategy described up to here was explained for a single polytopic obstacle. In the general case with p polytopes, this method must be applied to each one of them. As a result, one can obtain a set of equations in the form of (17). For convenience, we may join all these inequalities in an unique one:

$$-\mathbf{\Theta}_{\mathrm{k}}\mathbf{y}_{\mathrm{k}} \leq -\boldsymbol{\theta}_{\mathrm{k}}, \tag{18}$$

where $\mathbf{\Theta}_{\mathrm{k}} \in \mathbb{R}^{n_o \times 3}$ and $\boldsymbol{\theta}_{\mathrm{k}} \in \mathbb{R}^{n_o}$, with $n_o \in \mathbb{Z}_+$ corresponding to the number of perceived obstacles at instant k.

3.4 Reference Trajectory

The reference trajectory of MPC is calculated by two different ways: the conventional form, for the case of free flight (no obstacle near), and the decelerated form, which is used when at least one obstacle is being noticed by the quadrotor at current moment.

In the first case, the reference trajectory is a straight line towards $\mathbf{w}_{\mathrm{j}}$, traveled with constant speed ($\bar{v}$). Suppose that, at instant k, the current waypoint is $\mathbf{w}_{\mathrm{j}}$. The following equation describes this case:

$$\bar{\mathbf{y}}_{k+i|k} = \mathbf{y}_{\mathrm{k}} + \mathbf{n}_{\mathrm{k}}\bar{v}iT, \tag{19}$$

with
$\mathbf{n}_{\mathrm{k}} = \frac{\mathbf{w}_{\mathrm{j}} - \mathbf{y}_{\mathrm{k}}}{\|\mathbf{w}_{\mathrm{j}} - \mathbf{y}_{\mathrm{k}}\|}$,
for $i = 1, ..., N$. Note that the second term of the right-hand side of (19) is the product of a reference velocity vector with a time step. Moreover, one can see that the reference velocity has a magnitude $\bar{v}$ and points towards the direction of the current waypoint $\mathbf{w}_{\mathrm{j}}$.

In the second case, a constant deceleration is considered in the reference trajectory, as is given in the following equation:

$$\bar{\mathbf{y}}_{\mathrm{k+i|k}} = \mathbf{y}_{\mathrm{k}} + \mathbf{n}_{\mathrm{k}}\bar{v}iT + \mathbf{n}_{\mathrm{k}}\bar{a}\frac{(iT)^2}{2}, \tag{20}$$

where the constant acceleration $\bar{a}$ is calculated using the known Torricelli equation of kinematics:

$$\bar{a} = \frac{-\bar{v}^2}{2\|\mathbf{w}_{\mathrm{j}} - \mathbf{y}_{\mathrm{k}}\|}. \tag{21}$$

An exception to the two cases occurs when the vehicle reaches the final waypoint $\mathbf{w}_{\mathrm{q}}$. In this case, it is commanded to stay at $\mathbf{w}_{\mathrm{q}}$ by simply making

$$\bar{\mathbf{y}}_{k+i|k} = \mathbf{w}_{\mathrm{q}}, \tag{22}$$

for $i = 1, ..., N$.

The reference trajectory is considered by the MPC in the form of the augmented vector $\mathbf{Y}_{\mathrm{k}}$:

$$\bar{\mathbf{Y}}_{\mathrm{k}} \triangleq \left[\bar{\mathbf{y}}_{\mathrm{k+1|k}}^{\mathrm{T}} \ \bar{\mathbf{y}}_{\mathrm{k+2|k}}^{\mathrm{T}} \ \ldots \ \bar{\mathbf{y}}_{\mathrm{k+N|k}}^{\mathrm{T}}\right]^{\mathrm{T}}, \tag{23}$$

where, for $i = 1, ..., N$, $\bar{\mathbf{y}}_{\mathrm{k+i|k}}$ denotes the reference value for $\mathbf{y}_{\mathrm{k+i|k}}$.

i. Waypoint Commutation

For switching from the current waypoint $\mathbf{w}_{\mathrm{j}}$ to the next one $\mathbf{w}_{\mathrm{j+1}}$ of the waypoint sequence, we adopt the following rule. Let the system be initialized with the first waypoint $\mathbf{w}_1$ as the current one. Suppose now that at a certain instant k, the waypoint $\mathbf{w}_{\mathrm{j}}$ is the current one. Define the waypoint detection ball $\mathcal{B}_{\mathbf{w}_{\mathrm{j}}}(\lambda) \subset \mathbb{R}^3$ as being an Euclidian ball centered at $\mathbf{w}_{\mathrm{j}}$, with a radius λ. From now on, $\lambda \in \mathbb{R}$ is called the waypoint detection radius. Therefore, the commutation to the next waypoint $\mathbf{w}_{\mathrm{j+1}}$ of the waypoint sequence is realized, up to the last waypoint $\mathbf{w}_{\mathrm{q}}$, as soon as the following condition is verified:

$$\mathbf{y}_{\mathrm{k}} \in \mathcal{B}_{\mathbf{w}_{\mathrm{j}}}(\lambda). \tag{24}$$

3.5 Model Predictive Controller

i. Prediction Model

Denote the prediction horizon by $N \in \mathbb{Z}_+,\ N > 0$ and define the vector of output predicted values along it as

$$\mathbf{Y}_{\mathrm{k}} \triangleq \left[\mathbf{y}_{\mathrm{k+1|k}}^{\mathrm{T}} \ \mathbf{y}_{\mathrm{k+2|k}}^{\mathrm{T}} \ \ldots \ \mathbf{y}_{\mathrm{k+N|k}}^{\mathrm{T}}\right]^{\mathrm{T}} \in \mathbb{R}^{3N}. \tag{25}$$

Similarly, define the vector of future incremental inputs at instant k as

$$\Delta\mathbf{U}_{\mathrm{k}} \triangleq \left[\Delta\mathbf{u}_{\mathrm{k|k}}^{\mathrm{T}} \ \Delta\mathbf{u}_{\mathrm{k+1|k}}^{\mathrm{T}} \ \ldots \ \Delta\mathbf{u}_{\mathrm{k+N-1|k}}^{\mathrm{T}}\right]^{\mathrm{T}} \in \mathbb{R}^{3N}. \tag{26}$$

As presented in Maciejowski (2002), the prediction model can be obtained from the state-space model in equations (10)-(11). With this, the prediction equation can be written as

$$\mathbf{Y}_{\mathrm{k}} = \mathcal{F}\mathbf{z}_{\mathrm{k}} + \mathcal{G}\Delta\mathbf{U}_{\mathrm{k}}, \tag{27}$$

with

$$\mathcal{F} \triangleq \begin{bmatrix} \tilde{\mathbf{C}}\tilde{\mathbf{A}} \\ \tilde{\mathbf{C}}\tilde{\mathbf{A}}^2 \\ \vdots \\ \tilde{\mathbf{C}}\tilde{\mathbf{A}}^N \end{bmatrix} \in \mathbb{R}^{3N\times 9},\ \mathcal{G} \triangleq \begin{bmatrix} \tilde{\mathbf{C}}\tilde{\mathbf{B}} & \mathbf{0}_{3\times3} & \ldots & \mathbf{0}_{3\times3} \\ \tilde{\mathbf{C}}\tilde{\mathbf{A}}\tilde{\mathbf{B}} & \tilde{\mathbf{C}}\tilde{\mathbf{B}} & \ldots & \mathbf{0}_{3\times3} \\ \vdots & \vdots & \vdots & \vdots \\ \tilde{\mathbf{C}}\tilde{\mathbf{A}}^{N-1}\tilde{\mathbf{B}} & \tilde{\mathbf{C}}\tilde{\mathbf{A}}^{N-2}\tilde{\mathbf{B}} & \ldots & \tilde{\mathbf{C}}\tilde{\mathbf{B}} \end{bmatrix} \in \mathbb{R}^{3N\times 3N}.$$

ii. Constraints

Applying the constraints (14) and (17) to the predicted outputs $\mathbf{y}_{k+i|k}$, for $i = 1, ..., N$, one can write, respectively,

$$[\mathbf{r}_{\mathrm{min}}]_N \leq \mathbf{Y}_{\mathrm{k}} \leq [\mathbf{r}_{\mathrm{max}}]_N, \tag{28}$$

$$-\mathcal{O}\mathbf{Y}_{\mathrm{k}} \leq -[\boldsymbol{\theta}_{\mathrm{k}}]_N, \tag{29}$$

where $[a]_N$ denotes an extended vector with N copies of a and

$$\mathcal{O} \triangleq \begin{bmatrix} \mathbf{\Theta}_{\mathrm{k}} & \mathbf{0}_{n_o\times3} & \mathbf{0}_{n_o\times3} & \ldots & \mathbf{0}_{n_o\times3} \\ \mathbf{0}_{n_o\times3} & \mathbf{\Theta}_{\mathrm{k}} & \mathbf{0}_{n_o\times3} & \ldots & \mathbf{0}_{n_o\times3} \\ \vdots & \vdots & \vdots & \ldots & \vdots \\ \mathbf{0}_{n_o\times3} & \mathbf{0}_{n_o\times3} & \mathbf{0}_{n_o\times3} & \ldots & \mathbf{\Theta}_{\mathrm{k}} \end{bmatrix} \in \mathbb{R}^{n_o N\times 3N}.$$

Using (27), equations (28) and (29) can be rewritten in terms of $\Delta\mathbf{U}_{\mathrm{k}}$, yielding

$$[\mathbf{r}_{\mathrm{min}}]_N - \mathcal{F}\mathbf{z}_{\mathrm{k}} \leq \mathcal{G}\Delta\mathbf{U}_{\mathrm{k}} \leq [\mathbf{r}_{\mathrm{max}}]_N - \mathcal{F}\mathbf{z}_{\mathrm{k}}, \tag{30}$$

$$-\mathcal{O}\mathcal{G}\Delta\mathbf{U}_{\mathrm{k}} \leq -[\boldsymbol{\theta}_{\mathrm{k}}]_N + \mathcal{O}\mathcal{F}\mathbf{z}_{\mathrm{k}}. \tag{31}$$

It's necessary to write the constraint (13) in terms of $\Delta\mathbf{u}_{\mathrm{k}}$, in order to adjust it to the incremental formulation. From reference Maciejowski (2002), we obtain

$$\mathbf{U}_{\mathrm{k}} = [\mathbf{u}_{\mathrm{k-1}}]_N + \mathcal{T}_N\Delta\mathbf{U}_{\mathrm{k}}, \tag{32}$$

where

$$\mathcal{T}_N = \begin{bmatrix} \mathbf{I}_3 & \mathbf{0}_{3\times 3} & \dots & \mathbf{0}_{3\times 3} \\ \mathbf{I}_3 & \mathbf{I}_3 & \dots & \mathbf{0}_{3\times 3} \\ \vdots & \vdots & \dots & \vdots \\ \mathbf{I}_3 & \mathbf{I}_3 & \dots & \mathbf{I}_3 \end{bmatrix} \in \mathbb{R}^{3N\times 3N},\ \mathbf{U}_{\mathrm{k}} \triangleq \begin{bmatrix} \mathbf{u}_{\mathrm{k|k}} \\ \mathbf{u}_{\mathrm{k+1|k}} \\ \vdots \\ \mathbf{u}_{\mathrm{k+N-1|k}} \end{bmatrix} \in \mathbb{R}^{3N}.$$

Applying equation (32) in (13), we have

$$[\mathbf{u}_{\min}]_N \leq [\mathbf{u}_{\mathrm{k}-1}]_N + \mathcal{T}_N \Delta \mathbf{U}_{\mathrm{k}} \leq [\mathbf{u}_{\max}]_N\,, \tag{33}$$

Finally, equations (30), (31) and (33) can be immediately put into the form

$$\boldsymbol{\Xi}\Delta\mathbf{U}_{\mathrm{k}} \leq \boldsymbol{\xi}, \tag{34}$$

with

$$\boldsymbol{\Xi} \triangleq \begin{bmatrix} \mathcal{G} \\ -\mathcal{G} \\ -\mathcal{O}\mathcal{G} \\ \mathcal{T}_N \\ -\mathcal{T}_N \end{bmatrix} \in \mathbb{R}^{13N\times 3N},\ \boldsymbol{\xi} \triangleq \begin{bmatrix} [\mathbf{r}_{\max}]_N - \mathcal{F}\mathbf{z}_{\mathrm{k}} \\ -[\mathbf{r}_{\min}]_N + \mathcal{F}\mathbf{z}_{\mathrm{k}} \\ -[\boldsymbol{\theta}_{\mathrm{k}}]_N + \mathcal{O}\mathcal{F}\mathbf{z}_{\mathrm{k}} \\ [\mathbf{u}_{\max} - \mathbf{u}_{\mathrm{k}-1}]_N \\ -[\mathbf{u}_{\min} - \mathbf{u}_{\mathrm{k}-1}]_N \end{bmatrix} \in \mathbb{R}^{13N}.$$

iii. Computation of the Control Input

The optimal incremental input vector $\Delta\mathbf{u}^*$ consists of the first three elements of $\Delta\mathbf{U}_{\mathrm{k}}$ that minimizes the quadratic cost functional

$$\mathcal{J}(\Delta\mathbf{U}_{\mathrm{k}}) = \|\mathbf{Y}_{\mathrm{k}} - \bar{\mathbf{Y}}_{\mathrm{k}}\|^2 + \rho\|\Delta\mathbf{U}_{\mathrm{k}}\|^2, \tag{35}$$

subject to the constraints in equation (34), where $\rho \in \mathbb{R},\ \rho > 0$ is a design weighting parameter. Then, the optimal control input vector $\mathbf{u}^*_{\mathrm{k}}$ is obtained by $\mathbf{u}^*_{\mathrm{k}} = \mathbf{u}_{k-1} + \Delta\mathbf{u}^*_{\mathrm{k}}$.

The above problem can be immediately put into the format of a conventional quadratic optimization problem under linear inequality constraints. To solve this convex optimization problem, efficient numerical methods are available Boyd and Vandenberghe (2004).

iv. Computation of the Force Magnitude and Attitude Commands

As soon as the control input vector $\mathbf{u}^*_{\mathrm{k}}$ is computed, it can be converted into the corresponding thrust command $\bar{\mathbf{F}}_{\mathrm{k}}$ by using equation (7). However, this force command is not sufficient as an output of a guidance law for a multirotor aerial vehicle. In fact, the system has to provide two commands for the vehicle's internal control loops: a command for the magnitude of the total thrust vector and an attitude command. The complete explanation to understand how the controller compute these informations can be found in Prado and Santos (2014).

4. Simulation Results

This section aims to evaluate the proposed guidance method using computational simulations. Subsection 4.1 describes the simulation environment, while Subsection 4.2 presents the results collected.

4.1 System Simulation

The proposed guidance system was simulated in MATLAB/Simulink with a six-degree-of-freedom dynamics model of attitude and position, considering a quadrotor in "plus" configuration with the parameters listed in Tab. 1. As can be seen, some model's parameters were considered as uncertainties, which is the case of the inertia matrix, the force and moment constants of the rotors. These parameters were assumed to follow an uniform distribution of probability and the respective limits are given in Tab. 1.

Tabela 1: **Parameters simulated of the quadrotor vehicle.**

Mass: $m = 1$ kg
Inertia matrix: $J \in U(J_{\min}, J_{\max})$
Frame radius: $l = 0.2$ m
Motor-drive time constant: $\tau = 0.01$ s
Motor's maximum speed: $\omega_{\max} = 10000$ rpm
Rotor's force constant: $k_f \in U(2.09, 4.17)\cdot 10^{-5}$
Rotor's moment constant: $k_t \in U(5.00, 10.00)\cdot 10^{-7}$

where
$J_{\min} = \begin{bmatrix} 0.013 & -0.007 & -0.007 \\ -0.007 & 0.013 & -0.007 \\ -0.007 & -0.007 & 0.023 \end{bmatrix}$ kg $\cdot$ m^2 and $J_{\max} = \begin{bmatrix} 0.027 & 0.007 & 0.007 \\ 0.007 & 0.027 & 0.007 \\ 0.007 & 0.007 & 0.037 \end{bmatrix}$ kg $\cdot$ m^2.

In the (internal) attitude control loop, a saturated proportional-derivative control law with proportional gain $K_p = 20$ and derivative gain $K_d = 8$ is used. On the other hand, in the (external) position control loop, the MPC proposed in Section 3 is adopted. Tab. 2 presents the MPC parameters used in the simulations. From the values of $\mathbf{F}_{\text{min}}$ and $\mathbf{F}_{\text{max}}$, one can compute the maximum inclination command as $\bar{\varphi}_{\max} = 35$, the minimum thrust magnitude command as $\bar{F}_{\min} = 2$ N, and the maximum thrust magnitude command as $\bar{F}_{\max} = 20$ N.

Tabela 2: **Parameters of the MPC controller.**

Parameter
Prediction horizon: $N = 20$
Sampling time: $T = 0.1$ s
Control weight: $\rho = 5$
Reference speed: $\bar{v} = 3$ m/s
Waypoint detection radius: $\lambda = 0.5$ m
Obstacle perception radius: $\beta \in \{0, 1.5\}$ m
Minimum position: $\mathbf{r}_{\text{min}} = [-5 \;\; -5 \;\; -5]^{\text{T}}$ m
Maximum position: $\mathbf{r}_{\text{max}} = [30 \; 30 \; 4]^{\text{T}}$ m
Minimum thrust: $\mathbf{F}_{\text{min}} = [-1 \;\; -1 \; 2]^{\text{T}}$ N
Maximum thrust: $\mathbf{F}_{\text{max}} = [1 \; 1 \; 20]^{\text{T}}$ N

4.2 Results of Simulations

One trajectory with four waypoints was considered in an environment containing four polytopic obstacles. The chosen waypoints are: $\mathbf{w}_1 = [\; 1 \quad 1 \quad 1 \;]^{\text{T}}$, $\mathbf{w}_2 = [\; 12.5 \quad 1 \quad 1 \;]^{\text{T}}$ m, $\mathbf{w}_3 = [\; 12.5 \quad 13 \quad 1 \;]^{\text{T}}$ m and $\mathbf{w}_4 = [\; 1 \quad 13 \quad 1 \;]^{\text{T}}$ m. In addition, the quadrotor was subject to a variant disturbance force $\mathbf{F}_{\text{G}}^{\text{d}}$, simulating an environmental wind. This perturbation was modeled as a normal aleatory variable, so $\mathbf{F}_{\text{G}}^{\text{d}} \in N\left([\; 0 \quad 0 \quad 0 \;]^{\text{T}}\text{N}, [\; 0.10^2 \quad 0.10^2 \quad 0.07^2 \;]^{\text{T}}\text{N}^2\right)$.

In order to evaluate the proposed obstacle avoidance method, even in the presence of parametric uncertainties and aleatory disturbance force, the system was simulated in a Monte Carlo approach, with the total of 100 runs. At Fig. 3, one can see all the vehicle's trajectories obtained in this simulation.

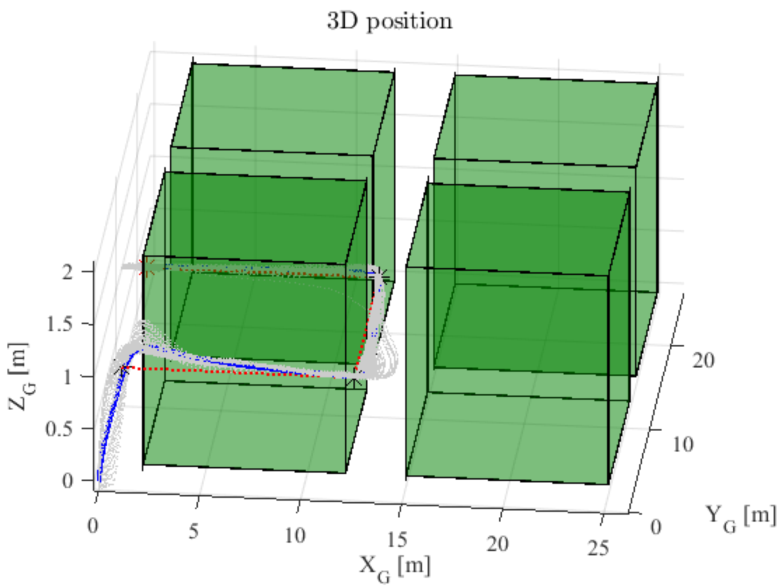

Figura 3: **Trajectories executed by the quadrotor in each realization of the Monte Carlo scheme (in gray). The continuous blue line illustrates the final average path of the vehicle. The waypoints are represented as asterisks and the desired trajectory is the dashed red line. The four polytopic obstacles are given in green.**

In next Fig. 4 (b), the previous trajectories are presented in a top view and so projected in the $X_{\text{G}} - Y_{\text{G}}$ plane. In Fig. 4 (a), are given the trajectories simulated in a similar scenario without obstacles (this is the case when $\beta = 0$ m). As can be seen in the left-side figure, the quadrotor flies inside the obstacles' limits in many cases. However, by the action of the obstacle avoidance scheme, one can see that all the trajectories in the right-side figure respect the four polytopes. This comparison attests the effectiveness of the method.

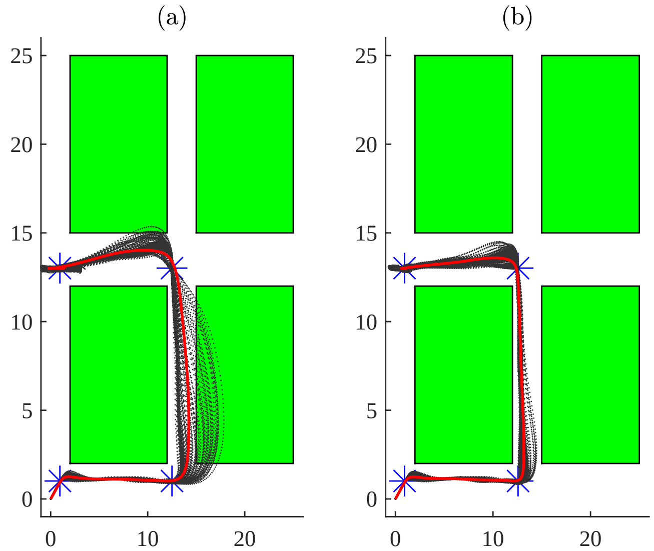

Figura 4: **Comparison between a case without using the obstacle avoidance approach (a) and one with this method on (b): the proposed strategy prevents collisions with the obstacles.**

Figures 5, 6 and 7 illustrates the operation of the MPC controller during the simulation. In the X_{G} and Y_{G} directions, where the control constraints are tighter, it's possible to verify that MPC respects these limitations in all the runs. In Z_{G} direction, in a different way, the predictive controller doesn't implement the extreme commands, due to the greater thrust capability along this direction.

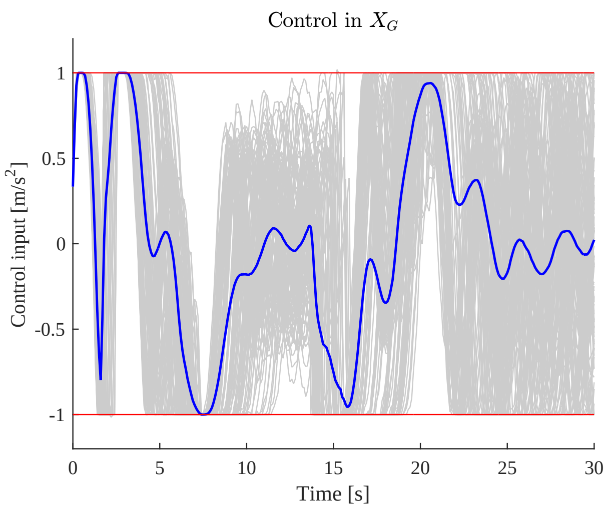

Figura 5: **Control calculated by MPC in X_{G} direction. The red lines represent the constraints imposed to the controller in this direction.**

Finally, Fig. 8 presents the variation of the multirotor's speed during all the Monte Carlo's tests. It can be clearly noticed the effect of the deceleration implemented when the vehicle is close to an obstacle. The three strong decelerations observed in the blue line are related to the second, third and fourth waypoint, respectively. The first two of them are caused by the obstacle avoidance method and the last is referred to the ending of the trajectory.

5. Conclusions

The present paper proposed a model predictive controller (MPC) for waypoint-based guidance with obstacle avoidance of multirotor aerial vehicles. The commands to the controller are a sequence of waypoints and a

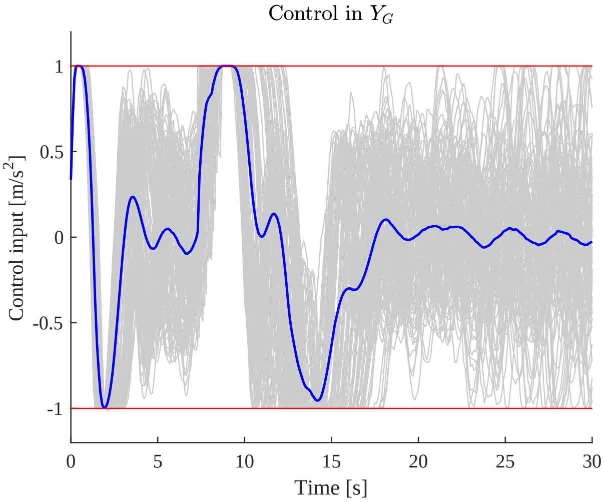

Figura 6: **Control calculated by MPC in Y_G direction. The red lines represent the constraints imposed to the controller in this direction.**

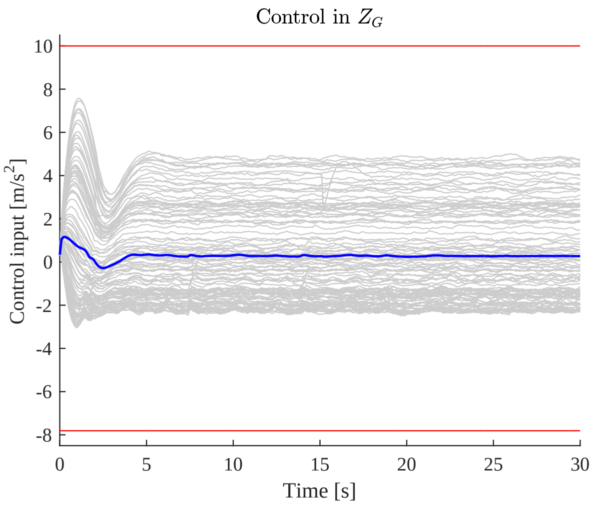

Figura 7: **Control calculated by MPC in Z_G direction. The red lines represent the constraints imposed to the controller in this direction.**

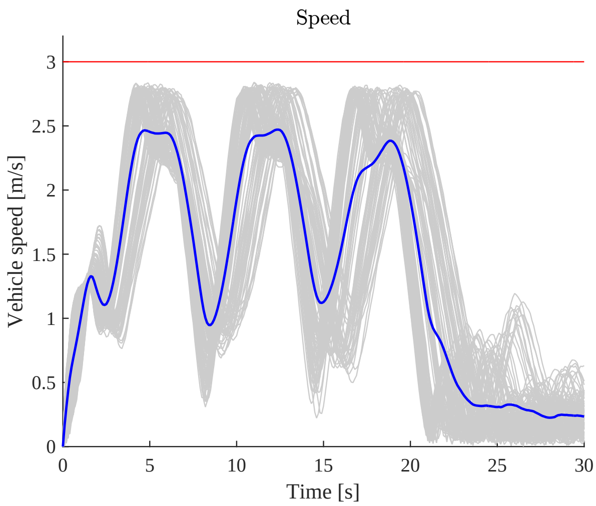

Figura 8: **Variation of the quadrotor's speed along the trajectories. The blue line illustrates the average variation of the speed. The red line indicates the reference velocity $\bar{v}$.**

reference speed. The proposed method is able to guide the vehicle along a desired trajectory respecting a set of constraints related to the environment, thrust force and obstacles. The obstacle avoidance strategy consists of constraining the optimization problem and decelerating the future reference trajectory of MPC when one obstacle enters into the perception sphere of the vehicle.

The simulations were done in a Monte Carlo approach, considering some parametric uncertainties and aleatory variation of the disturbance force. It was shown that, if the obstacle avoidance method was disabled, the vehicle would probably crashes against one of the polytopes. However, with the activation of the proposed strategy, the quadrotor could avoid the four obstacles and completed the path in all the cases. In addition, the effect of deceleration of the method was studied and it was verified the MPC observation to constraints in the control input.

6. REFERÊNCIAS

Alexis, K., Papachristos, C., Siegwart, R. and Tzes, A., 2014. "Robust Model Predictive Flight Control of Unmanned Rotorcrafts". In *European Control Conference (ECC)*. Strasbourg, France, pp. 498–503.

Almeida, F., 2008. "Waypoint navigation using constrained infinite horizon model predictive control". In *AIAA Guidance, Navigation and Control Conference and Exhibit*. Honolulu, Hawaii.

Boyd, S. and Vandenberghe, L., 2004. *Convex Optimization*. Cambridge University Press, New York.

Maciejowski, J.M., 2002. *Predictive Control with Constraints*. Harlow: Prentice Hall.

Prado, I.A.A. and Santos, D.A., 2014. "A Safe Position Tracking Strategy for Multirotor Helicopters". In *22st Mediterranean Conference on Control and Automation (MED)*. Palermo, Italy.

Raffo, G.V., Ortega, M.G. and Rubio, F.R., 2010. "An integral predictive/nonlinear $\mathcal{H}_\infty$ control structure for a quadrotor helicopter". *Automatica*, Vol. 46, No. 1, pp. 29–39.

Richards, A. and How, J.P., 2002. "Aircraft trajectory planning with collision avoidance using mixed integer linear programming". In *Proceedings of the American Control Conference*. Anchorage, USA.

Santos, D.A., Saotome, O. and Cela, A., 2013. "Trajectory control of multirotor helicopters with thrust vector constraints". In *21st Mediterranean Conference on Control and Automation*. Platanias, Greece.

Viana, I.B., Prado, I.A.A., Santos, D.A. and Goes, L.C.S., 2015. "Trajectory Tracking Control of an Aerial Robot with Obstacle Avoidance". In *11th IFAC Symposium on Robot Control*. Salvador, Brazil.

7. COPYRIGHT LIABILITY